Skyrmion stability at finite isospin chemical potential and temperature*

Wen-Li Yuan(苑文莉)[1;1)] Zhen-Ni Xu(徐珍妮)[1;2)] Jin-Li Zhang(张金利)[2;3)] Hong-Shi Zong(宗红石)[1,3,4;4)]

[1]Department of Physics, Nanjing University, Nanjing 210093, China
[2]Department of Physics and Jiangsu Key Laboratory for Numerical Simulation of Large Scale Complex Systems, Nanjing Normal University, Nanjing 210023, China
[3]Joint Center for Particle, Nuclear Physics and Cosmology, Nanjing 210093, China
[4]State Key Laboratory of Theoretical Physics, Institute of Theoretical Physics, CAS, Beijing 100190, China

Abstract: The skyrmion stability at finite isospin chemical potential μ_I is studied using the Skyrme Lagrangian with a finite pion mass m_π. A critical value $\mu_{Ic} = \sqrt{3/2}m_\pi$, above which a stable soliton does not exist, is found. We also explore some properties of the skyrmion as function of μ_I, i.e., the isoscalar rms radius and the isoscalar magnetic rms radius. Finally, considering the finite temperature effect on the skyrmion mass, we obtain a critical temperature T_c, using the profile function of the skyrmion, above which the skyrmion mass does not have a minimum, which can be interpreted as the occurrence of the deconfinement phase transition.

Keywords: skyrme model, isospin chemical potential, skyrmion stability

DOI: 10.1088/1674-1137/44/1/014103

1 Introduction

Physics of the hadronic matter with finite density and temperature has been a hot topic for a few decades [1-5]. It is now recognized that the phase diagrams of hadronic matter are much richer than what has been predicted by the perturbative quantum chromodynamics (QCD), and that phases of hadronic matter and their respective phase transitions might be realized in nature in various circumstances. There are two prominent topics, the evolution of the early Universe and the core of neutron stars, where the knowledge of the phase diagram would provide a much better understanding of the related phenomena.

There have been considerable developments concerning the phase diagram. The lattice QCD has provided much information about the finite temperature transitions, such as the value of the critical temperature and the form of the equation of state (EOS) [6-9]. However, in a system with finite chemical potential, the lattice QCD becomes invalid due to the "sign problem" [10].

As a consequence, various alternative effective models have been used, such as the Nambu-Jona-Lasinio (NJL) model [11-13] and the Dyson-Schwinger equations (DSEs) [14-18]. With these effective models, progress has been made in the study of the phase diagram. Furthermore, the phase structure of QCD at finite isospin chemical potential and zero baryon chemical potential with two light quarks was considered in Ref. [19]. In addition to the approaches based on the effective methods that include quarks as explicit degrees of freedom, effective field theories with hadronic fields only were also widely used [20-25].

In this work, we resort to the effective model which is expressed in terms of mesons and baryons that arise as topological objects — the Skyrme model [26]. This model has been widely used in the study of nucleons and nuclear matter, as well as in condensed matter physics (see Refs. [27-29] for reviews). In Ref. [30], Atiyah and Manton showed how to generate Skyrme field configurations from $SU(2)$ instantons by computing the holonomy along the lines parallel to the time axis. In Refs. [31, 32], the construction of Atiyah and Manton was extended, and the stability of skyrmions at finite temperature and the existence of a critical temperature $T_c$were discussed. It was shown that the skyrmion is no longer stable when $T > T_c$, and that this can be interpreted as the occurrence of the

Received 20 July 2019, Published online 22 November 2019

* Supported in part by Natural Science Foundation of China (NSFC) (11805097, 11535005, 11690030), and the Jiangsu Provincial Natural Science Foundation of China (BK20180323)

1) E-mail: wlyuan7@gmail.com
2) E-mail: jennie.phys@gmail.com
3) E-mail: jlzhang@njnu.edu.cn
4) E-mail: zonghs@nju.edu.cn

deconfinement phase transition. This phenomenon was also studied in the frame of the so-called hybrid model [33].

This paper is organized as follows. In Sec. 2, we study the skyrmion properties as function of isospin chemical potential at zero temperature. We find a critical isospin chemical potential $\tilde{\mu_I}_c \simeq 0.65$ above which the skyrmion breaks, and can therefore be regarded as the critical value for deconfinement. We also study the isoscalar rms radius and the isoscalar magnetic rms radius considering the effect of $\tilde{\mu_I}$. In Sec. 3, we study the effect of temperature on the skyrmion properties. We find that the mass of the skyrmion cannot attain a minimum when the temperature reaches a certain critical value, which can be interpreted as the deconfinement phase transition. We give a summary of our work in Sec. 4.

2 Finite isospin chemical potential and the skyrmion stability

We start from the Skyrme model with the pion mass term [34]

$$\begin{aligned}\mathcal{L} =&\frac{1}{16}F_\pi^2\mathrm{Tr}[\partial_\alpha U\partial^\alpha U^+]\\&+\frac{1}{32e^2}\mathrm{Tr}[[(\partial_\alpha U)U^+,(\partial_\beta U)U^+]^2]\\&+\frac{1}{8}m_\pi^2F_\pi^2(trU-2),\end{aligned}\tag{1}$$

where F_π is the pion decay constant, e is a numerical parameter, m_π is the pion mass and U is the $SU(2)$ matrix which transforms like $U\to AUB^+$ under $SU(2)\times SU(2)$. In this work, instead of their empirical values, we take $F_\pi = 108$ MeV and $e = 4.84$ which are obtained by fitting the nucleon mass and the Δ mass [34].

The isospin chemical potential can be introduced through the substitution [35, 36]

$$\partial_\alpha U\to D_\alpha U=\partial_\alpha U-\mathrm{i}\frac{\mu_I}{2}[\tau_3,U]g_{\alpha 0},\tag{2}$$

where τ is the third Pauli matrix and $g_{\alpha\beta}$ is the metric tensor in the Minkowski space.

The Skyrme model including the isospin chemical potential then becomes

$$\begin{aligned}\mathcal{L}(\mu_I) =&\mathcal{L}+\frac{\mu_I^2F_\pi^2}{64}\mathrm{Tr}\{\omega^2\}-\frac{{\mu_I}^2}{64e^2}\mathrm{Tr}\{[\omega,L_\alpha]^2\}\\&+\frac{\mathrm{i}\mu_IF_\pi^2}{16}\mathrm{Tr}\{\omega L_0\}-\frac{\mathrm{i}\mu_I}{8e^2}\mathrm{Tr}\{\omega L_\alpha[L_0,L_\alpha]\},\end{aligned}\tag{3}$$

where, $\omega=\tau_3-U\tau^3U^+$ and $L_\alpha=L_\alpha\equiv U^+\partial_\alpha U$.

To calculate the effect of the isospin chemical potential on the skyrmion properties, we take the probe approximation of the profile function, that is the following hedgehog ansatz for the skyrmion solution which is still valid

$$U=\exp(\mathrm{i}\vec{\tau}\cdot\hat{\boldsymbol{r}}F(r))=\cos F(r)+\mathrm{i}(\vec{\tau}\cdot\hat{\boldsymbol{r}})\sin F(r),\tag{4}$$

where $\vec{\tau}$ is the sigma matrix vector and $\hat{r}$ denotes the spatial unitary vector, $\hat{\boldsymbol{r}}^2=1$. The profile function $F(r)$ satisfies the boundary conditions

$$F(0)=\pi,\quad F(\infty)=0.\tag{5}$$

For convenience of calculations, we define the following dimensionless variables

$$\begin{aligned}&\tilde{r}=\frac{eF_\pi}{2}r,\quad \tilde{m_\pi}=\frac{2}{eF_\pi}m_\pi,\\&\tilde{\mu_I}=\frac{2}{eF_\pi}\mu_I,\quad \tilde{\kappa}=\frac{2\kappa}{eF_\pi}.\end{aligned}\tag{6}$$

We then obtain the dimensionless soliton mass as

$$\begin{aligned}\tilde{M}(\tilde{\mu_I})=\frac{4e}{F_\pi}M=&4\pi\int\mathrm{d}\tilde{r}\tilde{r}^2\Big[F'^2+2\frac{\sin^2F}{\tilde{r}^2}\left(1+F'^2\right)+\frac{\sin^4F}{\tilde{r}^4}\\&+2\tilde{m_\pi}^2(1-\cos F)-\frac{2}{3}\tilde{\mu_I}^2\sin^4F\left(1+F'^2\right)\\&-\frac{2}{3}\tilde{\mu_I}^2\frac{\sin^4F}{\tilde{r}^2}\Big],\end{aligned}\tag{7}$$

where M is the soliton mass. The minimization of $\tilde{M}(\tilde{\mu_I})$ leads to the following equation of motion of the skyrmion profile function $F(\tilde{r})$

$$F''\left[1+\frac{2\sin^2F}{\tilde{r}^2}\left(1-\frac{1}{3}\tilde{\mu_I}^2\tilde{r}^2\right)\right]+\frac{2F'}{\tilde{r}}\left(1-\frac{2\tilde{\mu_I}^2\sin^2F}{3}\right)-\frac{\sin 2F}{\tilde{r}^2}\left(1-F'^2\right)\left(1-\frac{1}{3}\tilde{\mu_I}^2\tilde{r}^2\right)-\frac{\sin^2F\sin 2F}{\tilde{r}^4}\left(1-\frac{2}{3}\tilde{\mu_I}^2\tilde{r}^2\right)-\tilde{m_\pi}^2\sin F=0.\tag{8}$$

Let us now analyze the behavior of the profile function for large distances. By considering $F(\infty)\to 0$, one has $\sin F(\tilde{r})\to F(\tilde{r})$ and $\cos F(\tilde{r})\to 1$, so that at large distances Eq. (8) reduces to the following form

$$F''+\frac{2F'}{\tilde{r}}-\left(\tilde{m_\pi}^2-\frac{2}{3}\tilde{\mu_I}^2+\frac{2}{\tilde{r}^2}\right)F=0.\tag{9}$$

From this equation one can easily obtain the critical value for $\tilde{\mu_I}_c=\sqrt{3/2}\tilde{m_\pi}\simeq 0.65$ ($\mu_{Ic}\simeq 170$ MeV). Eq. (9), which describes the behavior of $F(\tilde{r})$ at large distances, is a spherical Bessel equation which implies that the usual criteria for localized finite energy solutions [37] fail to be satisfied for $\tilde{\mu_I}>\tilde{\mu_I}_c$.

We plot in Fig. 1 the solution of the profile function for a few typical values of $\tilde{\mu_I}$. The plot clearly shows that localized solutions exist only for $\tilde{\mu_I}<\tilde{\mu_I}_c$. For $\tilde{\mu_I}>\tilde{\mu_I}_c$, we can still obtain solutions which behave as spherical

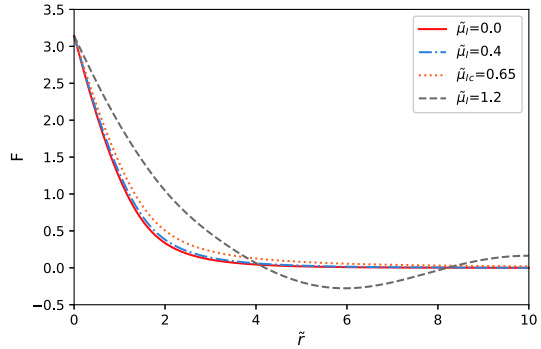

Fig. 1. (color online) Hedgehog profiles $F(\tilde{r})$ for various values of the isospin chemical potential $\tilde{\mu}_I$. The profiles $F(\tilde{r})$ are the exact solutions of Eq. (8) except the gray dashed curve. The red solid curve represents the solution for the isospin chemical potential $\tilde{\mu}_I = 0$, the blue dot-dashed curve is for $\tilde{\mu}_I = 0.4$, and the yellow dotted curve for $\tilde{\mu}_I = \sqrt{3/2}\tilde{m}_\pi \simeq 0.65$. The gray dashed curve, which behaves as a spherical Bessel function at large distances, is for $\tilde{\mu}_I = 1.2$, which is larger than the critical isospin chemical potential $\tilde{\mu}_{Ic}$, but is not a soliton solution which has localized finite energy. It is clearly seen that the isospin chemical potential has a distinct influence on the profile $F(\tilde{r})$ when $\tilde{\mu}_I > \tilde{\mu}_{Ic}$.

Bessel functions at large distances, but they are not soliton solutions which have localized finite energy. This suggests the occurrence of a phase transition — the deconfinement phase transition.

We also study the soliton mass as a function of the isospin chemical potential $\tilde{\mu}_I$ for the spherically symmetric hedgehog ansatz, presented in Fig. 2. When $\tilde{\mu}_I$ is larger than 0.65, the localized finite energy solutions of Eq. (8) no longer exist, and the soliton mass integral in Eq. (7) does not exist either.

We study next the relation between the other relevant physical quantities and the isospin chemical potential. It

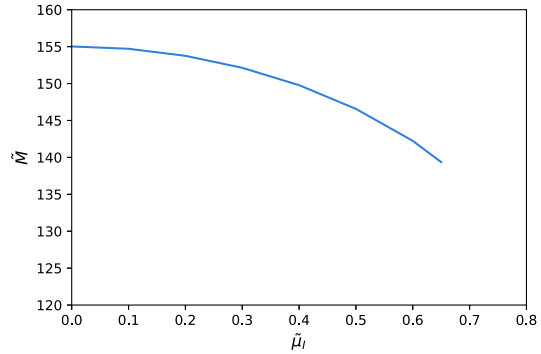

Fig. 2. (color online) The soliton mass as a function of the isospin chemical potential $\tilde{\mu}_I$ for the spherically symmetric hedgehog ansatz. For $\tilde{\mu}_I < 0.1$, the soliton mass is almost stable, while for $\tilde{\mu}_I > 0.1$ the soliton mass decreases with the increase of the isospin chemical potential. The curve stops at $\tilde{\mu}_{Ic} \simeq 0.65$, which is close to $\tilde{\mu}_{Ic} = \sqrt{3/2}\tilde{m}_\pi$.

is well know that the Skyrme model allows the existence of different conserved currents and respective charges, which can be used to define several effective radii. Thus, we can study these radii for finite isospin chemical potentials, which give additional information about the behavior close to the phase transition.

Here, we consider the isoscalar rms radius $\langle \tilde{r}^2 \rangle^{1/2}_{I=0}$ and the magnetic rms radius $\langle \tilde{r}^2 \rangle^{1/2}_{M,I=0}$, which are defined in the Skyrme model as

$$\langle \tilde{r}^2 \rangle^{1/2}_{I=0} = \sqrt{\int_0^\infty \mathrm{d}\tilde{r}\tilde{r}^2 \rho_B}, \tag{10}$$

$$\langle \tilde{r}^2 \rangle^{1/2}_{M,I=0} = \sqrt{\int_0^\infty \mathrm{d}\tilde{r}\tilde{r}^2 \rho^I_M(r)}, \tag{11}$$

where the baryon number density ρ_B and the isoscalar magnetic moment density ρ_M are

$$\rho_B = -\frac{2}{\pi}\sin^2 F(r)F'(r), \tag{12}$$

$$\rho_{M,I=0} = \frac{r^2 F' \sin^2 F}{\int_0^\infty \mathrm{d}r r^2 F' \sin^2 F}. \tag{13}$$

When the isospin chemical potential is turned on, we find from the Euler-Lagrange equation for the soliton profile $F(\tilde{r})$, Eq. (8), that the profile $F(\tilde{r})$ also acquires a dependence on $\tilde{\mu}_I$

$$F(\tilde{r}) \to F(\tilde{r},\tilde{\mu}_I). \tag{14}$$

Therefore, substituting the solution of Eq. (8) into Eq. (10) and Eq. (11), we obtain the dependence of the skyrmion radius on the isospin chemical potential.

We plot in Fig. 3 and Fig. 4 the dependence of the isoscalar rms radius and the isoscalar magnetic rms radius on $\tilde{\mu}_I$. From these figures we can see that when the isospin chemical potential exceeds the critical value $\tilde{\mu}_{Ic} \simeq 0.65$, both radii diverge, which suggests the occurrence of a phase transition. Furthermore, for $\tilde{\mu}_I > \tilde{\mu}_{Ic}$ loc-

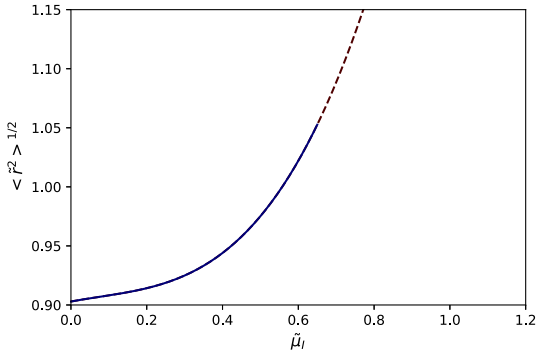

Fig. 3. (color online) $\langle \tilde{r}^2 \rangle^{1/2}_{I=0}$ as a function of $\tilde{\mu}_I$. For the isospin chemical potential $\tilde{\mu}_I > \tilde{\mu}_{Ic}$, the rms radius (the blue solid curve) diverges, which suggests the occurrence of a phase transition.

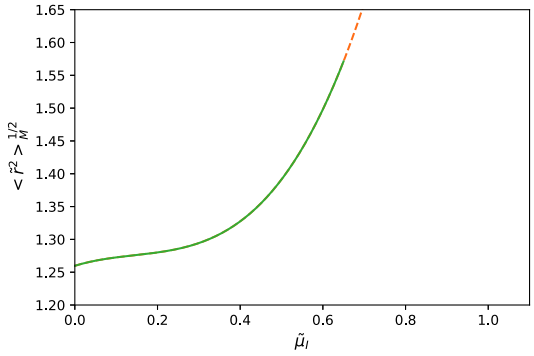

Fig. 4. (color online) $\langle \tilde{r}^2 \rangle^{1/2}_{M,I=0}$ as a function of $\tilde{\mu_I}$. For isospin chemical potential larger than 0.65, the rms radius diverges.

alized finite energy solutions do not exist and the radii cannot be obtained. However, in order to get some information about the behavior of the radii for large $\tilde{\mu_I}$, we extend our numerical calculations of Eq. (8), shown as dashed lines in the figures. Although we cannot formally prove that the radii diverge at the critical $\tilde{\mu_I} = \tilde{\mu_{Ic}}$, the numerical results support this claim.

Another physical quantity which indicates a phase transition occurs is the distribution of the baryon number density ρ_B. In Fig. 5, we plot ρ_B as a function of $\tilde{r}$. One can clearly see that the baryon density is localized for small isospin chemical potentials, but for $\tilde{\mu_I} \gtrsim \tilde{\mu_{Ic}}$, the skyrmion spreads in space and loses its identity as a soliton, although the baryon number remains unchanged. This transition is naturally considered as a signature of the decofinement phase transition [38].

We would like to clarify here that, as is known, the skyrmion is a topological soliton, which is in fact a topological defect. Above the critical isospin chemical potential, the stable skyrmion solution cannot exist. This is to say that the topological defect is not present anymore and that a deconfinement phase transition occured. Similarly to the Kosterlitz-Thouless (KT) phase transition [39-42],

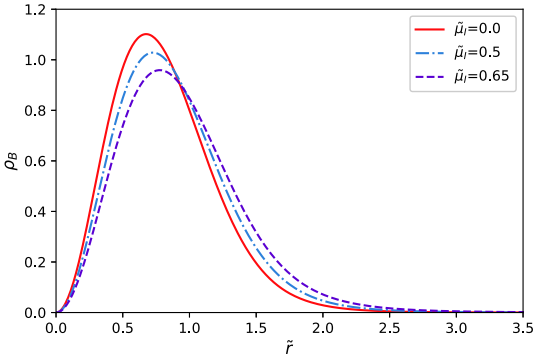

Fig. 5. (color online) The baryon number density ρ_B as a function of $\tilde{r}$ for typical values of the isospin chemical potential. The red solid curve is for the isospin chemical potential $\tilde{\mu_I} = 0$, the blue dot-dashed curve for $\tilde{\mu_I} = 0.5$, and the purple dashed curve for $\tilde{\mu_I} = 0.65$.

which is caused by the topological defect –vortex, this phase transition cannot be driven by symmetry breaking (or restoration). Therefore, there is no symmetry breaking pattern behind it.

3 Finite temperature effects and the skyrmion stability

The procedure to construct a skyrmion-like configuration from an $SU(2)$ instanton by computing the holonomy along the lines parallel to the time axis was studied by M. Atiyah and N. Manton [30]. This ansatz was later generalized to the thermal instanton in Ref. [31], in which the temperature effect is introduced by means of the skyrmion thermal profile

$$F(r) = \pi\left[1 - \frac{r + \frac{1}{2}\lambda^2(\kappa\coth(\kappa r) - 1/r)}{\sqrt{r^2 + \frac{1}{4}\kappa^2\lambda^4 + \kappa r\lambda^2\coth(\kappa r)}}\right], \qquad (15)$$

where $\kappa = 2\pi T$ and λ is the parameter in the thermal profile.

In terms of the dimensionless quantities given in Eq. (6), Eq. (15) can be rewritten as

$$F(\tilde{r}) = \pi\left[1 - \frac{\tilde{r} + \frac{1}{2}\tilde{\lambda}^2(\tilde{\kappa}\coth(\tilde{\kappa}\tilde{r}) - 1/\tilde{r})}{\sqrt{\tilde{r}^2 + \frac{1}{4}\tilde{\kappa}^2\tilde{\lambda}^4 + \tilde{\kappa}\tilde{r}\tilde{\lambda}^2\coth(\tilde{\kappa}\tilde{r})}}\right]. \qquad (16)$$

We plot in Fig. 6 the thermal profile for different temperatures and zero isospin chemical potential. From this plot, one can clearly see that under the influence of temperature, $F(\tilde{r})$ does not oscillate at large distances. This is in stark contrast to the hedgehog profiles $F(\tilde{r})$ presented in Fig. 1, where $F(\tilde{r})$ is shown to oscillate at large distances when the isospin chemical potential is larger than the critical value.

We study the effect of temperature on the skyrmion mass by substituting the profile $F(\tilde{r})$ into Eq. (7). For a fixed isospin chemical potential, we increase the value of the temperature, and when the temperature reaches a certain value T_c where $\tilde{M}(\tilde{\lambda},\tilde{\mu_I},T)$ as a function of $\tilde{\lambda}$ no longer has a minimum, one can conclude that this temperature is the critical temperature corresponding to the fixed isospin chemical potential. Then, for varying isospin chemical potentials, we can use the same method to get the corresponding critical temperature. We plot in Fig. 7 the skyrmion mass $\tilde{M}$ as a function of $\tilde{\lambda}$ for a fixed isospin chemical potential $\tilde{\mu_I} = 0.5$ and different temperatures. This figure shows that among the three skyrmion mass curves, the dashed dot line for $\tilde{\kappa}_c = 4.77$, which corresponds to the critical temperature $T_c = \kappa_c/2\pi$, does not have a minimum. In other words, localized finite energy solutions do not exist. This phenomenon is interpreted as

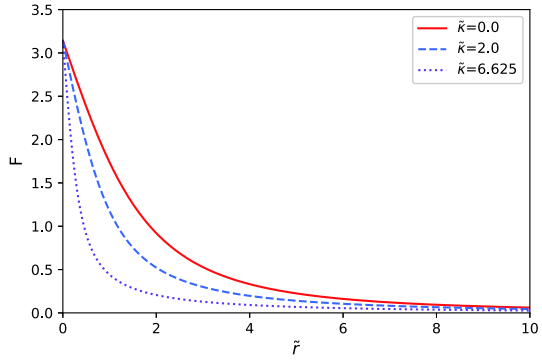

Fig. 6. (color online) The skyrmion thermal profile F as a function of $\tilde{r}$ at finite temperature and zero isospin chemical potential. The red solid curve is for the temperature $\tilde{\kappa}=0$, the blue dashed curve for $\tilde{\kappa}=2.0$, and the purple dotted curve for $\tilde{\kappa}=6.625$. Note that $\tilde{\kappa}=6.625$ is the critical temperature when the isospin chemical potential is zero.

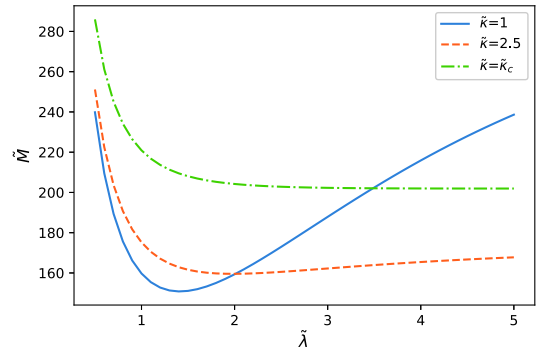

Fig. 7. (color online) The soliton mass $\tilde{M}(\tilde{\lambda},\tilde{\mu}_I,T)$ as a function of $\tilde{\lambda}$ in the spherically symmetric hedgehog ansatz and for $\tilde{\mu}_I=0.5$. The blue solid curve is the soliton mass for $\tilde{\kappa}=1.0$ ($\kappa=261.2$ MeV); the minimum $\tilde{M}=150.8$ ($M=841$ MeV) is at $\tilde{\lambda}=1.4$. The orange dashed curve is for $\tilde{\kappa}=2.5$ ($\kappa=653$ MeV) with the minimum $\tilde{M}=159.6$ at $\tilde{\lambda}=2.0$. The green dot-dashed line is for the critical temperature $\tilde{\kappa}_c=4.8$ (κ_c=1254 MeV) where the minimum does not exist.

the occurrence of the deconfining phase transition.

In Fig. 8 , we show the $\tilde{\mu}_I$ dependence of T_c. It can be seen that T_c decreases as $\tilde{\mu}_I$ increases. When $\tilde{\mu}_I \gtrsim \tilde{\mu}_{Ic}$, we could not find a soliton solution, i.e. a solution with a localized finite energy and finite temperature. Thus, we conclude that both the isospin chemical potential and the temperature contribute to the occurrence of instabilities in the skyrmion solution.

We would like to point out that the deconfinement phase transition in the skyrmion model cannot be described by the Landau symmetry breaking theory. Thus, the order of deconfinement phase transition cannot be investigated by the traditional Landau phase theory, which is different from the Polyakov loop. It is well known that although the center symmetry is explicitly broken by quarks in the fundamental representation, the Polyakov

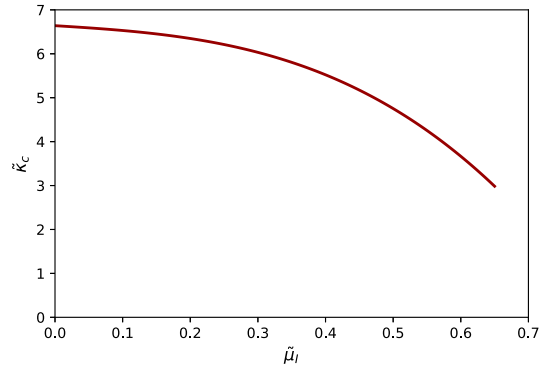

Fig. 8. (color online) The dependence of the critical temperature $\tilde{\kappa}$ on the isospin chemical potential $\tilde{\mu}_I$ in the spherically symmetric hedgehog ansatz.

loop is still used to study the deconfinement phase transition in the Polyakov loop extended NJL model, which is similar to the chiral phase transition with explicitly broken term for finite current quark mass. Furthermore, the deconfinement phase transition is described in this study by the topological defect, so that the order of the phase transition cannot be defined.

4 Summary and conclusions

In this work, we have studied the behavior of skyrmion properties on the isospin chemical potential $\tilde{\mu}_I$. After analyzing the behavior of the profile function $F(\tilde{r})$ for large distances, and of the numerical skyrmion mass evolution and soliton solutions, we found that there is a critical value $\tilde{\mu}_{Ic}$ above which the localized finite energy solutions no longer exist, with $\tilde{\mu}_{Ic}=\sqrt{3/2}\tilde{m}_\pi$ in the spherically symmetric hedgehog ansatz. We also presented the behavior of the isoscalar rms radius $\left\langle\tilde{r}^2\right\rangle_{I=0}^{1/2}$ and the isoscalar magnetic rms radius $\left\langle\tilde{r}^2\right\rangle_{M,I=0}^{1/2}$ for several isospin chemical potentials, and found that for isospin chemical potential above the critical value $\tilde{\mu}_{Ic}\backsimeq 0.65$ both radii are divergent, as shown in Fig. 3 and Fig. 4. We have also considered the effect of the finite temperature following M. Atiyah and N. Manton, and found a critical temperature which minimizes the skyrmion mass in terms of T and $\tilde{\lambda}$ that can be interpreted as the deconfining phase transition. In Fig 7, it was shown that for a particular value $\tilde{\mu}_I=0.5$ the minimum of the skyrmion mass increases with temperature, and that there exists a critical temperature above which the minimum disappears. The dependence of the critical temperature T_c on $\tilde{\mu}_I$ was shown in Fig. 8. In our study, we considered the skyrmion solution as a topological defect, which is the result of quantum fluctuations of the ground state. As the isospin chemical potential increases, quantum fluctuations are enhanced. For large isospin chemical potentials, the quantum fluctu-

ations are strong enough to break the stability of the topological defects, and the skyrmion solutions no longer exist leading to the deconfinement phase transition. As the reason behind the skyrmion approach is to have an effective representation of baryons, the existence of such a phase transition is quite interesting.

We would like to thank Zhu-Fang Cui and Yong-Liang Ma for their constructive comments and reading through the manuscript. Z.-F.C. also helped to conceive the idea.

References

1 W. Cassing and E. Bratkovskaya, Phys. Rept., **308**: 65 (1999)
2 A. Sedrakian, Prog. Part. Nucl. Phys., **58**: 168 (2007)
3 R. S. Hayano and T. Hatsuda, Rev. Mod. Phys., **82**: 2949 (2010)
4 J. W. Holt, M. Rho, and W. Weise, Physics Reports, **621**: 2 (2016)
5 A. Hosaka, T. Hyodo, K. Sudoh et al, Prog. Part. Nucl. Phys., **96**: 88 (2017)
6 J. B. Kogut and D. K. Sinclair, Phys. Rev. D, **66**: 034505 (2002)
7 T. Bhattacharya, M. I. Buchoff, N. H. Christ et al (HotQCD Collaboration), Phys. Rev. Lett., **113**: 082001 (2014)
8 H.-T. Ding, O. Kaczmarek, and F. Meyer, Phys. Rev. D, **94**: 034504 (2016)
9 S. Borsanyi, Z. Fodor, J. N. Guenther et al, Nucl. Phys. A, **982**: 223 (2019)
10 S. Ejiri and N. Yamada, Phys. Rev. Lett., **110**: 172001 (2013)
11 S. P. Klevansky, Rev. Mod. Phys., **64**: 649 (1992)
12 H. Kohyama, D. Kimura, and T. Inagaki, Nucl. Phys. B, **896**: 682 (2015)
13 J.-L. Zhang, C.-M. Li, and H.-S. Zong, Chinese Phys. C, **42**: 123105 (2018)
14 C. D. Roberts and A. G. Williams, Prog. Part. Nucl. Phys., **33**: 477 (1994)
15 P. Maris and C. D. Roberts, Int. J. Mod. Phys. E, **12**: 297 (2003)
16 I. C. Cloët and C. D. Roberts, Prog. Part. Nucl. Phys., **77**: 1 (2014)
17 Z.-F. Cui, I. C. Cloët, Y. Lu et al, Phys. Rev. D, **94**: 071503 (2016)
18 B.-L. Li, Z.-F. Cui, B.-W. Zhou et al, Nucl. Phys. B, **938**: 298 (2019)
19 D. T. Son and M. A. Stephanov, Phys. Rev. Lett., **86**: 592 (2001)
20 B. A. Campbell, J. Ellis, and K. A. Olive, Nucl. Phys. B, **345**: 57 (1990)
21 D. K. Hong, Phys. Lett. B, **473**: 118 (2000)
22 M. Harada and K. Yamawaki, Phys. Rev. D, **64**: 014023 (2001)
23 M. D'Elia and M.-P. Lombardo, Phys. Rev. D, **67**: 014505 (2003)
24 M. Harada, F. Sannino, and J. Schechter, Phys. Rev. D, **69**: 034005 (2004)
25 M. Harada, C. Sasaki, and W. Weise, Phys. Rev. D, **78**: 114003 (2008)
26 T. Skyrme, Nucl. Phys., **31**: 556 (1962)
27 I. Zahed and G. E. Brown, Phys. Rept., **142**: 1 (1986)
28 G. Brown and M. Rho, World Scientific (2016)
29 Y.-L. Ma and M. Rho, Sci. China Phys. Mech. Astron., **60**: 032001 (2017)
30 M. Atiyah and N. Manton, Phys. Lett. B, **222**: 438 (1989)
31 K. J. Eskola and K. Kajantie, Zeitschrift für Physik C Particles and Fields, **44**: 347 (1989)
32 J. Dey and J. Eisenberg, Phys. Lett. B, **334**: 290 (1994)
33 H. Falomir, M. Loewe, and J. Rojas, Phys. Lett. B, **300**: 278 (1993)
34 G. S. Adkins and C. R. Nappi, Nucl. Phys. B, **233**: 109 (1984)
35 H. A. Weldon, Phys. Rev. D, **26**: 1394 (1982)
36 A. Actor, Phys. Lett. B, **157**: 53 (1985)
37 D. J. Wallace, Physics Bulletin, **34**: 29 (1983)
38 T. Sakai and H. Suganuma, Phys. Lett. B, **430**: 168 (1998)
39 T. J. Sluckin and A. Poniewierski, Phys. Rev. Lett., **55**: 2907 (1985)
40 M. Gräter and C. Wetterich, Phys. Rev. Lett., **75**: 378 (1995)
41 K. Moon, H. Mori, K. Yang et al, Phys. Rev. B, **51**: 5138 (1995)
42 P. A. Murthy, I. Boettcher, L. Bayha et al, Phys. Rev. Lett., **115**: 010401 (2015)